

Fragment Molecular Orbital Molecular Dynamics with the Fully Analytic Energy Gradient

Kurt R. Brorsen, Noriyuki Minezawa, Feng Xu, Theresa L. Windus, and Mark S. Gordon*

Department of Chemistry and Ames Laboratory, Iowa State University, Ames, Iowa 50011, United States

ABSTRACT: Fragment molecular orbital molecular dynamics (FMO-MD) with periodic boundary conditions is performed on liquid water using the analytic energy gradient, the electrostatic potential point charge approximation, and the electrostatic dimer approximation. Compared to previous FMO-MD simulations of water that used an approximate energy gradient, inclusion of the response terms to provide a fully analytic energy gradient results in better energy conservation in the NVE ensemble for liquid water. An FMO-MD simulation that includes the fully analytic energy gradient and two body corrections (FMO2) gives improved energy conservation compared with a previously calculated FMO-MD simulation with an approximate energy gradient and including up to three body corrections (FMO3).

1. INTRODUCTION

1.1. Fragment Molecular Orbital Method. Much progress has been made recently in improving algorithms for *ab initio* calculations on large systems.^{1,2} One strategy is to use a fragmentation approach, in which a large system of interest is divided into smaller subsystems, and *ab initio* calculations are performed on these smaller subsystems.² One of the most successful and extensively developed fragmentation methods is the fragment molecular orbital (FMO) method³ proposed by Kitaura et al. in 1999. The FMO method has been implemented for most *ab initio* and density functional theory (DFT) methods.^{4–8} Numerous approximations to the original FMO method have been implemented to improve the efficiency of the calculation. The two most important of these approximations are the electrostatic point charge (ESP-PC) approximation and the electrostatic dimer (ES-DIM) approximation.⁹ The ESP-PC approximation calculates the FMO embedded electrostatic potential using point charges rather than two electron integrals, while the ES-DIM approximation calculates the dimer energy of two fragments using point charges rather than using *ab initio* methods.

FMO gradients were developed soon after the introduction of the FMO method.¹⁰ Improvements to the gradient followed that allowed the use of gradients with the ESP-PC approximation¹¹ and the ES-DIM approximation.¹² Because the dimer (or trimer) density is not iterated to self-consistency, the FMO2 (or FMO3) method is not variational. Consequently, response terms arising from the derivative of the molecular orbital coefficients with respect to nuclear coordinates must be included in the calculation of the first derivative. Because the inclusion of these response terms in the gradient requires the solution of the coupled perturbed Hartree–Fock equations, the original formulation of the FMO gradient neglected the response terms, based on the supposition that such terms make only small contributions to the gradient. Nagata et al.¹³ solved these analytic gradient response equations for the FMO method at the restricted Hartree–Fock (RHF) level of theory (without the use of the ESP-PC approximation) by introducing the self-consistent Z-vector (SCZV) procedure. More recently, the response

equations have been solved for and implemented for FMO-MP2¹⁴ and for the general FMO method in which the ESP-PC approximation is included.¹⁵ The corresponding analytic gradients for FMO-DFT will be forthcoming shortly.

1.2. FMO Molecular Dynamics. Komeiji et al. first implemented FMO2-molecular dynamics (FMO-MD) in 2003,^{16,17} and many applications of FMO-MD have since been published.^{18–22} The authors of the first implementation of FMO-MD¹⁶ noted that the neglect of the response terms in the FMO gradient led to less than perfect energy conservation for a NVE ensemble, but this lack of energy conservation was deemed acceptable. Since the fully analytic gradient had yet to be derived, there was no alternative.

Further improvements to the FMO-MD algorithm have been implemented, both to the FMO-MD method itself and to improve the energy conservation of FMO-MD.²³ The FMO3 method, in which explicit three body interactions are included in the FMO calculation, improves both the total energy and electron density of a FMO calculation.^{24–26} This prompted the development of a FMO3-MD method to study water and protonated water systems²⁷ since three-body effects are important in water.²⁸ Although fully analytic FMO3 gradients have not yet been derived and implemented, it appears that using the FMO3 level of theory improves energy conservation in FMO-MD simulations.²³ Of course, while the FMO3 method is more accurate than FMO2 due to the explicit inclusion of three-body terms, it is likewise much more computationally demanding. It was recently demonstrated that FMO3-MD simulations (without periodic boundary conditions) are more than a factor of 4 more computationally expensive than a corresponding FMO2-MD simulation for water.²³ The inclusion of periodic boundary conditions will greatly increase this FMO3/FMO2 ratio, as many more calculations would have to be performed on triads of fragments when periodic boundary conditions are used. Therefore, from

Special Issue: Berny Schlegel Festschrift

Received: September 10, 2012

Published: October 11, 2012

the perspective of computational expense, FMO2-MD is preferable if the accuracy of its energetics and forces is adequate. This is especially the case if one can guarantee good FMO2-MD energy conservation.

Another addition to FMO-MD in an attempt to improve energy conservation is dynamic fragmentation.^{23,29,30} Dynamic fragmentation continually fragments a system over the course of a MD simulation, using a distance-based cutoff, and allows FMO-MD to describe processes such as proton transfer or chemical reactions. Dynamic fragmentation apparently improves energy conservation in FMO-MD simulations for systems such as a protonated water clusters.²³ While dynamic fragmentation seems to be beneficial for improving energy conservation for reactive systems, it is desirable to be able to run FMO-MD simulations without the need for dynamic fragmentation in order to reduce the complexity of FMO-MD runs.

All of the FMO-MD improvements described above have been implemented using a gradient that neglects the response terms. As noted above, the response terms for the FMO2-RHF method were recently derived and implemented using the SCZV procedure.¹³ As analytic gradients are essential for accurate MD simulations, these response terms should be included in all FMO-MD calculations. In the original derivation of the SCZV procedure, the root-mean-square deviation error of the analytic gradient with response terms was shown¹³ to improve the accuracy (measured by comparison to numerical gradients) for a single geometry by more than an order of magnitude, relative to the gradient in which the response terms are omitted. The new fully analytic gradient has also been combined with the effective fragment potential³¹ to perform the first FMO-MD simulation with response terms included in the gradient.³² These simulations showed good energy conservation.

The original implementation of the SCZV procedure assumed that the ESP-PC approximation was not used. This assumption severely restricts the use of the SCZV procedure for FMO-MD applications, since the ESP-PC approximation is normally applied in FMO calculations. Recently, Nagata et al.¹⁵ solved for and implemented the response terms for the FMO gradient within the ESP-PC approximation. This improvement to the gradient allows accurate FMO-MD simulations to be performed, with all common FMO approximations implemented and available. With this recent improvement, it is shown here that accurate FMO-MD simulations, including periodic boundary conditions, are possible without the need to use the FMO3-MD level of theory.

2. EQUATIONS OF FRAGMENT MOLECULAR ORBITAL METHOD

In the following, a brief overview of the FMO2 restricted Hartree–Fock (RHF) energy is presented. Details and equations for the FMO gradient^{10–13,15} and the FMO-MD method^{16,17,23} can be found elsewhere.

The FMO2 energy for RHF is

$$E = \sum_I E'_I + \sum_{I>J} (E'_{IJ} - E'_I - E'_J) + \sum_{I>J} \text{Tr}(\Delta \mathbf{D}^{IJ} \mathbf{V}^{IJ}) \quad (1)$$

where N is the number of fragments, I and J are monomer fragments, IJ is a dimer consisting of fragments I and J , E'_X is the internal fragment energy, \mathbf{V}^{IJ} is the matrix of the

electrostatic potential, and $\Delta \mathbf{D}^{IJ}$ is the dimer density difference matrix.

The internal fragment energy, E'_X , is

$$E'_X = \sum_{\mu\nu \in X} D_{\mu\nu}^X h_{\mu\nu}^X + \frac{1}{2} \sum_{\mu\nu\lambda\sigma \in X} \left[D_{\mu\nu}^X D_{\lambda\sigma}^X - \frac{1}{2} D_{\mu\lambda}^X D_{\nu\sigma}^X \right] \times (\mu\nu|\lambda\sigma) + E_X^{\text{NR}} \quad (2)$$

where $h_{\mu\nu}$ is the one-electron Hamiltonian of fragment X , E_X^{NR} is the nuclear repulsion potential energy of fragment X ,

$$E_X^{\text{NR}} = \sum_{B \in X} \sum_{A(\in X) > B} \frac{Z_A Z_B}{R_{AB}} \quad (3)$$

$D_{\lambda\sigma}^K$ is the density matrix element of fragment K , and $(\mu\nu|\lambda\sigma)$ is a two-electron integral in the AO basis. The elements of \mathbf{V}^{IJ} are expressed as

$$V_{\mu\nu}^{IJ} = \sum_{K \neq IJ} (u_{\mu\nu}^K + v_{\mu\nu}^K) \quad (4)$$

The one-electron and two electron terms in eq 4 are, respectively,

$$u_{\mu\nu}^K = \sum_{A \in K} \langle \mu | \frac{-Z_A}{|\mathbf{r} - \mathbf{R}_A|} | \nu \rangle$$

$$v_{\mu\nu}^K = \sum_{\lambda\sigma \in K} D_{\lambda\sigma}^K (\mu\nu|\lambda\sigma) \quad (5)$$

The dimer density difference matrix $\Delta \mathbf{D}^{IJ}$ is defined as

$$\Delta \mathbf{D}^{IJ} = \mathbf{D}^{IJ} - (\mathbf{D}^I \oplus \mathbf{D}^J) \quad (6)$$

For distances R_{XK} between a monomer or dimer X and a fragment K in the ESP, which are greater than a user defined value $R_{\text{ESP-PC}}$, the two electron terms in the electrostatic potential are approximated as point charges:

$$v_{\mu\nu}^K \cong \bar{v}_{\mu\nu}^K = \sum_{A \in K} \left\langle \mu \left| \frac{Q_A}{|\mathbf{r} - \mathbf{R}_A|} \right| \nu \right\rangle \quad (7)$$

where A is atom A in fragment K , Q_A is the nuclear charge on atom A , \mathbf{R}_A is coordinate of atom A , \mathbf{r} is the coordinate of fragment K , and μ and ν are atomic basis functions. This approximation is called the ESP-PC approximation and is used in most FMO calculations.

For a dimer IJ , if the monomer pair I and J are farther apart than the (user defined) value of $R_{\text{ES-DIM}}$, the dimer energy is approximated as

$$E'_{IJ} \cong E'_I + E'_J + \text{Tr}(\mathbf{D}^I \mathbf{u}^J) + \text{Tr}(\mathbf{D}^J \mathbf{u}^I) + \sum_{\mu\nu \in I} \sum_{\lambda\sigma \in J} D_{\mu\nu}^I D_{\lambda\sigma}^J (\mu\nu|\lambda\sigma) + \Delta E_{IJ}^{\text{NR}} \quad (8)$$

This approximation is called the ES-DIM approximation and reduces the number of *ab initio* dimer calculations that must be performed. The ES-DIM approximation is employed for most FMO calculations.

3. COMPUTATIONAL METHODS

A system of 32 water molecules was used to examine the accuracy of FMO-MD simulations with the ESP-PC approximation and response terms included in the gradient. This system was prepared by generating a random initial

configuration of 32 waters inside a box (box length = 9.865 Å), so that the density of the system matched that of water at 300 K. To equilibrate this system, a 50 ps classical MD simulation using the NVT ensemble at 300 K with a 0.5 fs step size was then performed using the previous random initial configuration as the starting point, and with randomized initial velocities so that the system temperature was 300 K. The force field used for the classical MD simulation was the general effective fragment potential (EFP2) method.^{33,34}

The final geometry produced by the classical MD equilibration was used as the initial geometry for the FMO-MD equilibration. The FMO-MD equilibration was performed using the NVT ensemble for 500 fs with a 1.0 fs step size and with randomized initial velocities to ensure that the temperature was maintained at 300 K. The Nose–Hoover thermostat with chains³⁵ was used to control the temperature. The velocity was randomized to a temperature of 300 K every 100 fs. For this FMO-MD equilibration, the ESP-PC approximation was not used, and the cutoff value for the ES-DIM approximation was set to 1.5: if monomers *I* and *J* are more than 1.5 reduced distances, ρ_{IJ} , apart, then the *ab initio* dimer calculation is not performed, and the interaction between fragments *I* and *J* is approximated using point charges. The reduced distance is

$$\rho_{IJ} = r_{IJ}/(R_I + R_J) \quad (9)$$

In eq 9, r_{IJ} is the Euclidean distance between fragments *I* and *J*, and R_X is the van der Waals radius of fragment *X*. The response terms were included in the energy gradient. All waters in the FMO-MD equilibration were treated at the RHF/6-31G(d,p) level of theory.

The final configuration and velocities of the FMO-MD equilibration were then used as the initial configuration and velocities for FMO-MD simulations using the NVE ensemble to examine the accuracy of the recent FMO gradient improvements. These FMO-MD simulations were performed at the RHF/6-31G(d,p) level of theory for 50 ps using time steps in a range from 0.25 to 1.5 fs. Cutoff values were set to 4.75 for the ESP-PC approximation and 1.5 for the ES-DIM approximation, so that these approximations were used if two fragments are more than 4.75 and 1.5 reduced distances away, respectively. Two different FMO-MD simulations were performed at each time step—one simulation that included the response terms in the gradient and one that neglected the response terms.

For all FMO-MD calculations in this study, periodic boundary conditions (PBC) using the minimum image convention were employed.³⁶ Previous studies²³ of energy conservation for FMO-MD lacked PBC and instead employed a harmonic potential *U* that constrained the system to remain within a sphere centered at the origin:

$$U = K[\max(\mathbf{r} - \mathbf{r}_c, 0)]^2 \quad (10)$$

where *K* is a force constant (set to 0.75 kcal/mol/Å² in the study), *r* is the distance to the origin, and r_c is the radius of the sphere. It is assumed in the present study that the use of PBC vs the harmonic potential has no noticeable relative effect on energy conservation for the FMO-MD simulations. Previous studies²³ have shown that no dynamic fragmentation occurs for systems of pure water, so no dynamic fragmentation was employed. All FMO-MD simulations in this study were performed using the General Atomic and Molecular Electronic Structure System (GAMESS).^{37,38}

The root-mean-square deviation of the total energy, $\text{RMSD}(E)$, was calculated for each of the FMO-MD NVE simulations as

$$\text{RMSD}(E) = \sqrt{\langle (E - \langle E \rangle)^2 \rangle} \quad (11)$$

The velocity-Verlet method was used to integrate the equations of motion in this study. For the velocity-Verlet method, the $\text{RMSD}(E)$ is proportional to the square of the time step, Δt .³⁹

$$\text{RMSD}(E) \propto (\Delta t)^2 \quad (12)$$

Therefore, a log–log graph of $\text{RMSD}(E)$ versus Δt should be linear with a slope of 2. This relationship was previously^{16,23,32} used to evaluate the ability of FMO-MD simulations to produce an accurate NVE ensemble and will also be used for this study.

4. RESULTS AND DISCUSSION

The log–log plot of $\text{RMSD}(E)$ versus Δt is shown in Figure 1. Benchmarking fully molecular orbital molecular dynamics

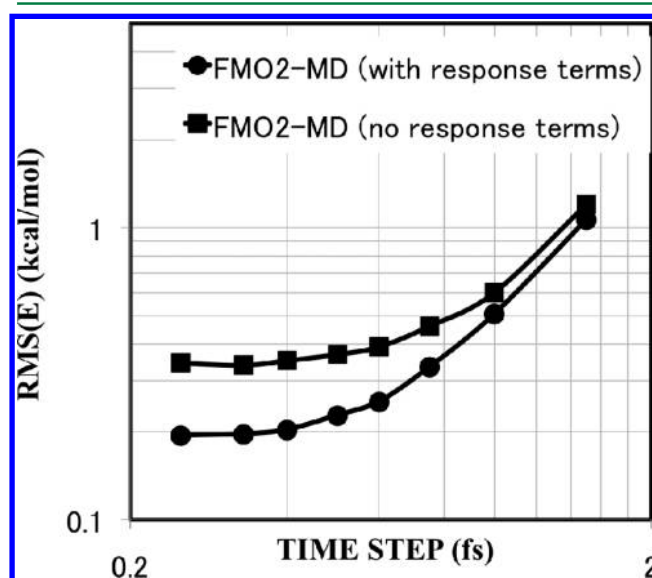


Figure 1. Log–log plot of the $\text{RMSD}(E)$ vs Δt for FMO2-MD with and without response terms as performed in this study.

(MO-MD) simulations, in which MD is performed using *ab initio* methods with no fragmentation, was not performed in this study due to the computational cost of performing MO-MD with PBC. Previous FMO-MD studies of water^{16,17,23} that have used MO-MD simulations as a benchmark have shown that MO-MD exhibits a smaller $\text{RMSD}(E)$ for a given time step than FMO-MD, for all variations of FMO-MD that were available at the time. It is therefore assumed in this study that with identical initial conditions, a smaller $\text{RMSD}(E)$ for a given MD simulation is always closer to the MO-MD value and therefore more accurate. Previous studies²³ have also shown that the velocity-Verlet integrator begins to fail for MO-MD simulations with a large time step and have therefore focused on the time step range of 0.25–1.0 fs, for which the MO-MD simulations have consistently shown perfect energy conservation based on a log–log plot of $\text{RMSD}(E)$ versus Δt with a slope of 2.

The FMO2-MD plot in Figure 1 demonstrates a significant improvement in energy conservation when the response terms are included in the energy gradient. Both simulations with and

without response terms included show a decrease in energy conservation over the time step range of 0.25–0.4 fs, but the FMO2-MD simulation with the response terms included is still more robust than is the FMO2-MD simulation without response terms. For larger step sizes Δt , the $\text{RMSD}(E)$ values for the two sets of simulations begin to converge at ~ 1.5 fs. The energy conservation begins to fail for both sets of MD simulations in the range of 0.25–0.4 fs. On the other hand, for the time step range in which most FMO-MD simulations will likely be performed (0.4–1.0 fs), a least-squares line of best fit to the data has a slope of 1.948 for the FMO2-MD simulations that includes response terms versus a slope of 0.772 for the FMO2-MD simulations that lack response terms. As a MD simulation exhibiting perfect energy conservation would have a best fit line with a slope of 2.0, the slopes of the best fit lines of the FMO2-MD simulations illustrate the necessity of adding response terms to the FMO gradient in order to obtain robust FMO2-MD simulations. In addition to showing better energy conservation, the energy drift of the FMO2-MD simulations (not shown) improves by over a factor of 3 when response terms are included in the gradient, for 800 FMO-MD 0.75 fs time steps on the system in this study.

Even with the response terms added, the $\text{RMSD}(E)$ becomes constant at small time step values, indicating that residual errors remain in the FMO gradient. These residual errors are likely due to the fragmentation employed by the FMO method and are inherent to any FMO-MD simulation. These residual errors could be further reduced by including higher body corrections to the FMO method (FMO3, FMO4, etc.) The residual errors would be completely eliminated at the limit of a full *ab initio* calculation on the entire system without fragmentation. Indeed, the reduction in residual errors with the addition of higher body corrections is seen in Figure 2 where the FMO3-MD results appear to trend to a smaller constant than FMO2-MD results.

The results presented in Figure 1 for the FMO2-MD simulation without response terms have a shape that is qualitatively similar to that of the previous FMO2-MD results²³ that are presented in Figure 2. As these two FMO2-MD

simulations are performed on identical systems of 32 waters at the RHF/6-31G(d,p) level of theory, these curves should in theory have the same $\text{RMSD}(E)$ values, but this is not the case. The FMO2-MD simulation (with no response terms) performed in the present work has a higher $\text{RMSD}(E)$ for a given time step than the previous study. This difference in the $\text{RMSD}(E)$ is due to differences in how the classical and FMO-MD equilibrations were performed and the use of different initial geometries and velocities for the FMO2-MD simulations. However, the $\text{RMSD}(E)$ differences between the two curves is less important than how closely the slope of each curve aligns with a line of slope 2. Also important is the relative shape of each curve with regard to the degree of energy conservation. From this perspective, both of the FMO2-MD simulations without response terms show similar, if not identical, energy conservation. Therefore, the FMO2-MD simulations without response terms can be treated as similar to one another.

Now, recall that the FMO2-MD and FMO3-MD curves in Figure 2 were computed without the response terms. Comparing the curves in Figure 1 with those in Figure 2, the curve for the FMO2-MD simulation with the response terms included appears to show a greater improvement over the FMO2-MD curve without response terms than does the FMO3-MD curve in Figure 2. This can be seen by examining the ratio of $\text{RMSD}(E)$ values for the FMO2-MD simulations with and without response terms in Figure 1 and the ratio of $\text{RMSD}(E)$ values for the FMO3-MD and FMO2-MD simulations, both without response terms in Figure 2. These comparisons are presented in Table 1. It is assumed that the

Table 1. Ratio of the $\text{RMSD}(E)$ for Various FMO2-MD Time Steps with and without Response Terms (Performed in This Study) and for FMO3-MD and FMO2-MD Both without Response Terms Performed in a Previous Study²³

time step (fs)	FMO2-MD without response terms/FMO2-MD with response terms	FMO2-MD/FMO3-MD
0.25	1.77	1.85
0.5	1.62	1.58
0.75	1.38	1.23
1.0	1.19	1.09
1.5	1.13	1.06

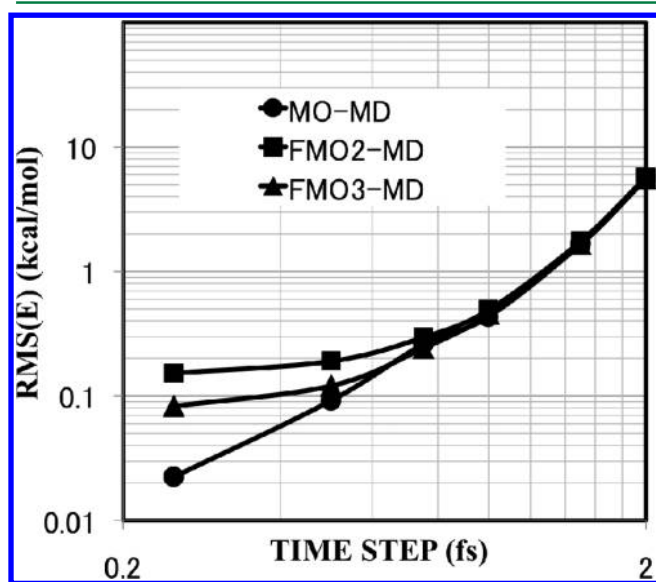


Figure 2. Log–log plot of the $\text{RMSD}(E)$ vs Δt for FMO2-MD and FMO3-MD without response terms and MO-MD from a previous study.²³

two FMO2-MD curves without response terms in Figures 1 and 2 can be treated as essentially the same, differing only due to different initial conditions. Therefore, referring to time steps in the range 0.4–1.0 fs in Table 1, the ratio for the FMO2-MD simulations with vs without response terms is slightly greater than the corresponding ratio for FMO3 vs FMO2, both without response terms. This suggests that the energy conservation improves at least as much by including response terms in FMO2-MD simulations as it does by choosing FMO3 without response terms. When one considers the additional computational expense incurred by choosing FMO3, FMO3-MD is a logical choice only when the system demands it due to the superior description of energetics and electron density of FMO3. It is also important to emphasize that FMO3-MD without a fully analytic gradient is not guaranteed to provide acceptable energy conservation, and therefore acceptable predictions of bulk properties, in all cases.

5. CONCLUSIONS AND FUTURE STUDIES

Accurate gradients are essential for producing correct forces in MD simulations. This can be seen for MD simulations with incomplete or inaccurate gradients, in which case energy conservation is violated for the NVE ensemble. For the FMO method, accurate gradients require the addition of the response terms obtained from the SCZV procedure. Therefore, it is necessary to include the response terms for all FMO-MD simulations. This practice has not been consistently followed in previous FMO-MD applications,^{19,21,22} in part because the fully analytic gradients have only recently been made available. Response terms for the FMO-MP2 gradient have been shown to improve the accuracy of the FMO-MP2 gradient even more than the corresponding response terms for the FMO-RHF method.¹⁴ Therefore, for FMO-MD simulations that include electron correlation, the addition of the response terms will be even more important than it is for FMO-RHF MD simulations. To date, response terms have not been implemented for other correlated *ab initio* methods. The response terms for FMO-DFT will be presented in a future paper. The lack of response terms for FMO interfaced with other *ab initio* methods limits the potential applications of FMO-MD for these methods, so solving for these response terms is a promising future research direction. Additionally, response terms have yet to be derived for FMO3. Since FMO3 is necessary for an accurate description of some systems and for FMO-MD with smaller time steps, the derivation and implementation of these response terms would be beneficial for future FMO-MD studies.

AUTHOR INFORMATION

Corresponding Author

*E-mail: mark@si.msg.chem.iastate.edu.

Notes

The authors declare no competing financial interest.

ACKNOWLEDGMENTS

This work was supported in part by a National Science Foundation Petascale Applications grant and in part by a Department of Energy Chemistry End Station grant, both to M.S.G. and T.L.W. K.R.B. is supported by a U.S. Department of Energy Computational Science Graduate Fellowship. The authors are grateful for the inspirational work by Professor Berny Schlegel in the field of analytic gradients and potential energy surfaces. The authors also thank Yuto Komeiji for graciously providing FMO-MD data from ref 23.

REFERENCES

- (1) *Linear-Scaling Techniques in Computational Chemistry and Physics*; Zalesny, R.; Papadopoulos, M. G.; Mezey, P. G.; Leszczynski, J., Eds.; Springer: Berlin, 2011.
- (2) Gordon, M. S.; Fedorov, D. G.; Pruitt, S. R.; Slipchenko, L. V. *Chem. Rev.* **2012**, *112*, 632.
- (3) Kitaura, K.; Ikeo, E.; Asada, T.; Nakano, T.; Uebayasi, M. *Chem. Phys. Lett.* **1999**, *313*, 701.
- (4) Fedorov, D. G.; Kitaura, K. *J. Chem. Phys.* **2004**, *121*, 2483.
- (5) Mochizuki, Y.; Yamashita, K.; Fukuzawa, K.; Takematsu, K.; Watanabe, H.; Taguchi, N.; Okiyama, Y.; Tsuboi, M.; Nakano, T.; Tanaka, S. *Chem. Phys. Lett.* **2010**, *493*, 346.
- (6) Fedorov, D. G.; Kitaura, K. *J. Chem. Phys.* **2010**, *123*, 134103.
- (7) Sugiki, S. I.; Kurita, N.; Sengoku, Y.; Sekino, H. *Chem. Phys. Lett.* **2003**, *382*, 611.
- (8) Fedorov, D. G.; Kitaura, K. *Chem. Phys. Lett.* **2004**, *389*, 129.
- (9) Nakano, T.; Kaminuma, T.; Sato, T.; Fukuzawa, K.; Akiyama, Y.; Uebayasi, M.; Kitaura, K. *Chem. Phys. Lett.* **2002**, *351*, 475.
- (10) Kitaura, K.; Sugiki, S. I.; Nakano, T.; Komeiji, Y.; Uebayasi, M. *Chem. Phys. Lett.* **2001**, *336*, 163.
- (11) Nagata, T.; Fedorov, D. G.; Kitaura, K. *Chem. Phys. Lett.* **2009**, *475*, 124.
- (12) Nagata, T.; Fedorov, D. G.; Kitaura, K. *Chem. Phys. Lett.* **2010**, *492*, 302.
- (13) Nagata, T.; Brorsen, K.; Fedorov, D. G.; Kitaura, K.; Gordon, M. S. *J. Chem. Phys.* **2011**, *134*, 124115.
- (14) Nagata, T.; Fedorov, D. G.; Li, H.; Kitaura, K. *J. Chem. Phys.* **2012**, *136*, 204112.
- (15) Nagata, T.; Fedorov, D. G.; Kitaura, K. *Chem. Phys. Lett.* **2012**, *544*, 87.
- (16) Komeiji, Y.; Nakano, T.; Fukuzawa, K.; Ueno, Y.; Inadomi, Y.; Nemoto, T.; Uebayasi, M.; Fedorov, D. G.; Kitaura, K. *Chem. Phys. Lett.* **2003**, *372*, 342.
- (17) Komeiji, Y.; Inadomi, Y.; Nakano, T. *Comput. Biol. Chem.* **2004**, *28*, 155.
- (18) Komeiji, Y.; Mochizuki, Y.; Nakano, T.; Fedorov, D. G. *J. Mol. Struct.: THEOCHEM* **2009**, *898*, 2.
- (19) Mochizuki, Y.; Komeiji, Y.; Ishikawa, T.; Nakano, T.; Yamataka, H. *Chem. Phys. Lett.* **2007**, *437*, 66.
- (20) Fedorov, D. G.; Ishida, T.; Kitaura, K. *J. Phys. Chem. A* **2005**, *109*, 2638.
- (21) Sato, M.; Yamataka, H.; Komeiji, Y.; Mochizuki, Y.; Ishikawa, T.; Nakano, T. *J. Am. Chem. Soc.* **2008**, *130*, 2396.
- (22) Komeiji, Y.; Ishikawa, T.; Mochizuki, Y.; Yamataka, H.; Nakano, T. *J. Comput. Chem.* **2009**, *30*, 40.
- (23) Komeiji, Y.; Mochizuki, Y.; Nakano, T. *Chem. Phys. Lett.* **2010**, *484*, 380.
- (24) Fedorov, D. G.; Kitaura, K. *J. Chem. Phys.* **2004**, *120*, 6832.
- (25) Fedorov, D. G.; Kitaura, K. *Chem. Phys. Lett.* **2006**, *433*, 182.
- (26) Fujita, T.; Fukuzawa, K.; Mochizuki, Y.; Nakano, T.; Tanaka, S. *Chem. Phys. Lett.* **2009**, *478*, 295.
- (27) Fedorov, D. G.; Kitaura, K. *J. Chem. Phys.* **2004**, *120*, 6832.
- (28) Xantheas, S. S. *Chem. Phys.* **2000**, *258*, 225.
- (29) Mochizuki, Y.; Komeiji, Y.; Ishikawa, T.; Nakano, T.; Yamataka, H. *Chem. Phys. Lett.* **2007**, *437*, 66.
- (30) Komeiji, Y.; Ishikawa, T.; Mochizuki, Y.; Yamataka, H.; Nakano, T. *J. Comput. Chem.* **2009**, *30*, 40.
- (31) Gordon, M. S.; Slipchenko, L.; Li, H.; Jensen, J. H. *Annu. Rep. Comput. Chem.* **2007**, *3*, 177.
- (32) Nagata, T.; Fedorov, D. G.; Kitaura, K. *J. Mol. Struct.: THEOCHEM* **2012**, *131*, 1136.
- (33) Day, N. P.; Jensen, H. J.; Gordon, M. S.; Webb, P. S. *J. Chem. Phys.* **1996**, *105*, 1968.
- (34) Gordon, M. S.; Freitag, M. A.; Bandyopadhyay, P.; Jensen, J. H.; Kairys, V.; Stevens, W. J. *J. Phys. Chem.* **2001**, *105*, 293.
- (35) Harvey, S. C.; Tan, R. K. Z.; Cheatham, T. E., III. *J. Comput. Chem.* **1998**, *19*, 726.
- (36) Fujita, T.; Nakano, T.; Tanaka, S. *Chem. Phys. Lett.* **2011**, *506*, 112.
- (37) Schmidt, M. W.; Baldridge, K. K.; Boatz, J. A.; Elbert, S. T.; Gordon, M. S.; Jensen, J. H.; Koseki, S.; Matsunaga, N.; Nguyen, K. A.; Su, S.; Windus, T. L.; Dupuis, M.; Montgomery, J. A. *J. Comput. Chem.* **1993**, *14*, 1347.
- (38) Gordon, M. S.; Schmidt, M. W. *Theory and Applications of Computational Chemistry, the First Forty Years*; Elsevier: Amsterdam, 2005.
- (39) Haile, J. M. *Molecular Dynamics Simulation — Elementary Methods*; Wiley: New York, 1992.